EVIDENCE OF WIND-INDUCED SUMMERTIME COASTAL UPWELLING AT GRAYS HARBOR, WASHINGTON

Kent S. Short

Seattle Ocean Services Unit
National Weather Service, NOAA
1700 Westlake Avenue, North
Seattle, WA 98109

Abstract

Winds and sea-surface temperatures (SST) at Grays Harbor, Washington are examined for a three-week period during summer 1978 to determine if wind-induced coastal upwelling is a readily-observable occurrence along the Washington coast. A coastal upwelling index is computed using the observed winds, and 24-hour running means of the upwelling index and SST are compared. This comparison indicates to a high degree of confidence that the SST does respond to the wind forcing, with a lag of approximately 60 hours. An analysis of infrared satellite and synoptic ship data substantiate the evidence that upwelling was present during this period.

I. INTRODUCTION

A frequently-neglected aspect of meteorology is its crucial interrelationship with its sister science, oceanography. This paper describes by means of a case study one example of this interrelationship, the phenomenon of coastal upwelling.

Coastal upwelling is an oceanic occurrence which has been observed in many areas of the world. Most notable among these areas are the waters along the western coasts of Africa, South America, and North America. This phenomenon is wind-driven in nature, owing its existence to the wind stress/Coriolis effect interaction first described by Ekman (1905). The net effect of a persistent wind blowing over a stretch of ocean is the development of an integrated mass transport in the wind-driven layer 90^{o} to the right (left) of the wind direction in the Northern Hemisphere (Southern Hemisphere). Consequently, a prevailing equatorward-blowing wind along the western coast of a continent (either hemisphere) will set up a net offshore water movement in the surface waters. To replace this water moving offshore, cold water from deeper layers moves upward inshore. See Figure 1. Coastal upwelling is most pronounced during the summer and early fall seasons, as might be expected, since that is the time when the subtropical high pressure centers are farthest poleward and most intense, producing prevailing equatorward winds along the continental west coasts.

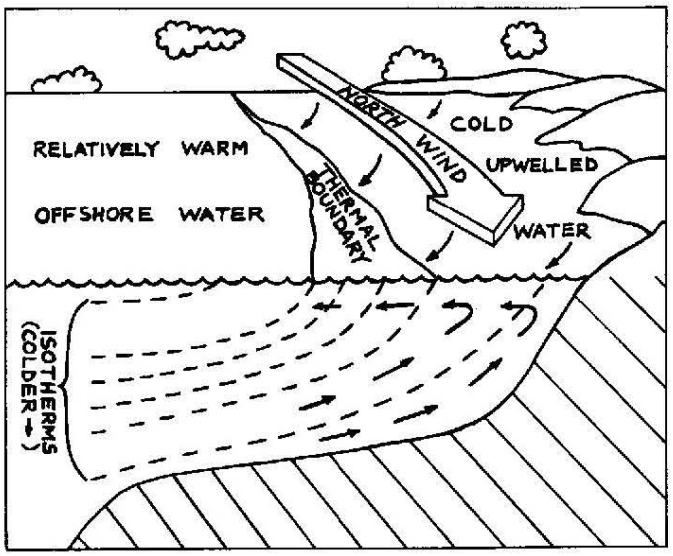

Figure 1. Schematic diagram of coastal upwelling.

Coastal upwelling has tremendous biological ramifications. The cold water upwelled from below is rich in nutrients, which porvide the necessary materials for a plentifully-supplied food chain. Regions affected by this phenomenon are among the most productive ocean areas in the world, and variations in the intensity of upwelling can have great economic impact on the world's protein market. It should be noted that recent investigations have shown that such variations in upwelling (i.e. the Peruvian "El Nino") can be predicted in

advance through application of statistical climatology (Quinn, et al, 1978).

The regional climatologist and coastal weather forecaster should also be aware of the upwelling phenomenon, as the presence of the cold upwelled water along the coast can strongly influence the airmass above it, and through advection can alter the local weather many miles inland. [See Mommsen (1978), for example.] A familiar example to West Coast forecasters is the frequent occurrence of summertime stratus along the California coast, which, in addition to the stabilizing influence of the Eastern Pacific Subtropical High, owes its existence partially to the condensation which occurs when warm moist air moves over the cold upwelled water and is cooled from below.

As mentioned previously, the west coast of North America is one of the principal areas of coastal upwelling. Upwelling along the coast of California and Oregon has been particularly well documented, since it is most intense in those areas. For examples of such studies, see: Halpern (1974); Huyer et al (1975); Mooers et al (1975); and Smith (1974). Although less frequently and intensely, the coast of Washington is also affected by summertime upwelling, though little verification for that assertion has previously existed. The following analysis is an attempt to provide some of that verification.

II. ANALYSIS

A three-week period beginning July 26, 1978 was studied using data from Grays Harbor Coast Guard Station at Westport, Washington. This period was chosen because it included two distinct wind shifts, starting out southwesterly, turning to primarily northwesterly (favorable for upwelling) for about ten days, then returning to southwesterly (see Figure 2a). Sea-surface temperatures (measured at the pier at the Coast Guard Station, approximately 3 n.mi. inside the harbor entrance) were examined for this period to investigate the relationship between the winds and the water temperature. The wind was measured at a well-exposed anemometer about 0.6 n.mi. from the ocean beach.

In order to quantify the comparison between the wind and water temperature, a numerical upwelling index was computed using the observed winds. This index, developed by Andrew Bakun of the Pacific Environmental Group of the National Marine Fisheries Service, NOAA [Bakun (1973)], is a computed mass transport of water normal to the coastline, based on Ekman transport theory (Ekman, 1905). The index is given by the equation:

$$U = .288 \frac{V^2}{\sin \phi} \cos (D-C + 270^\circ \quad (1)$$

where

V = wind speed (knots)
ϕ = latitude (deg)
D = wind direction (deg)
C = coastline normal (directed offshore) (deg)

The units of U are cubic meters per second per 100 meters of coastline. Positive values indicate offshore surface water movement (resulting in upwelling). Negative values indicate onshore surface water movement (resulting in downwelling). The theory from which Equation 1 is derived is briefly outlined in Appendix A.

In order to minimize the effects of diurnal wind changes and SST fluctuations due to tidal current reversals, a 24-hour running mean (8 observations) statistical filter was applied to the upwelling index and SST data. It should be noted that there are two observations (0600Z and 0900Z) each day which are not taken at Grays Harbor. These gaps are evident in the wind vector time series (Figure 2a). However, in order to perform a running mean in the upwelling index and SST values, it was necessary to interpolate these missing observations. Simple linear interpolation was used.

Ekman theory and several recent investigations [Cannon (1972); Thompson and O'Brien (1973); Stevenson et al (1974)] indicate that a lag exists between the onset of favorable winds for upwelling and the definite observance of the phenomenon. Estimates of this lag generally range between one and three days. Since the observation point for this study was inside Grays Harbor, it was felt a further lag might exist due to the additional time involved in mixing the cold upwelled water along the coast into the estuary. Consequently, several lag correlations were run on the upwelling index and SST running mean time series. Correlations for lags in the SST of 0, 36, 48, 57, 60, 63, and 72 hours were computed (limited computational facilities did not allow an exhaustive lag survey). Table 1 summarizes the lag correlations. At zero lag, a negligible correlation existed (r = -0.05). The maximum absolute value of the lag correlation coefficient was found for lags in the SST of 57 and 60 hours (r = -0.73). This is significant at the 99% confidence level based on a t-test of significance of the correlation coefficient. Figure 2 shows the wind vector time series, the corresponding 24-hour running mean upwelling index, and the 24-hour running mean SST (lagged by 60 hours). Note the visually evident approximate inverse correlation between the latter two.

In addition to the wind and SST data presented above, an Ocean Thermal Boundary Analysis (a Seattle Ocean Services Unit product) for August 8 is included (Figure 3) to show that synoptic ship

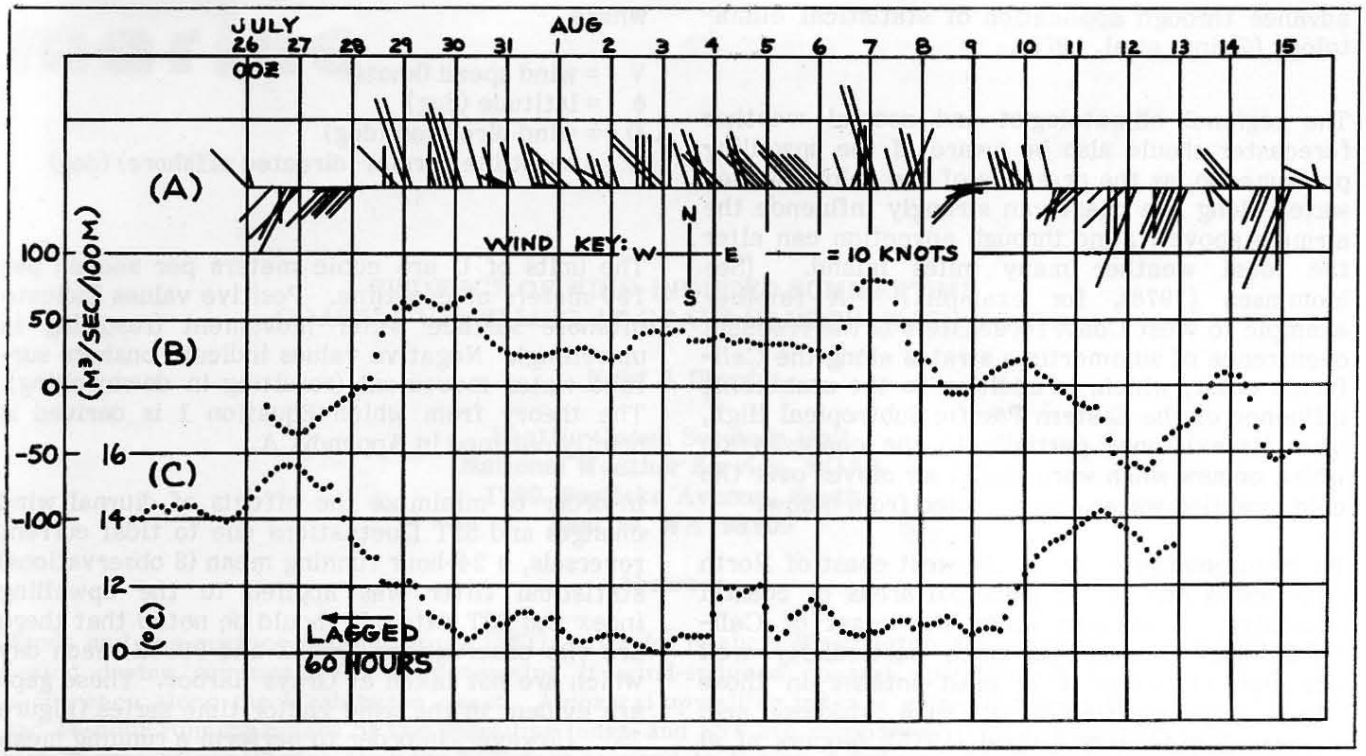

Figure 2. (A) Time series of Grays Harbor vector winds. (B) 24 hour running mean Grays Harbor upwelling index. (c) 24 hour running mean Grays Harbor SST (lagged by 60 hours).

LAG IN SST (HR)	CORRELATION COEFFICIENT
0	-0.05
36	-0.53
48	-0.68
57	-0.73
60	-0.73
63	-0.72
72	-0.70

TABLE 1. Summary of lag correlations (lagged SST vs. upwelling index)

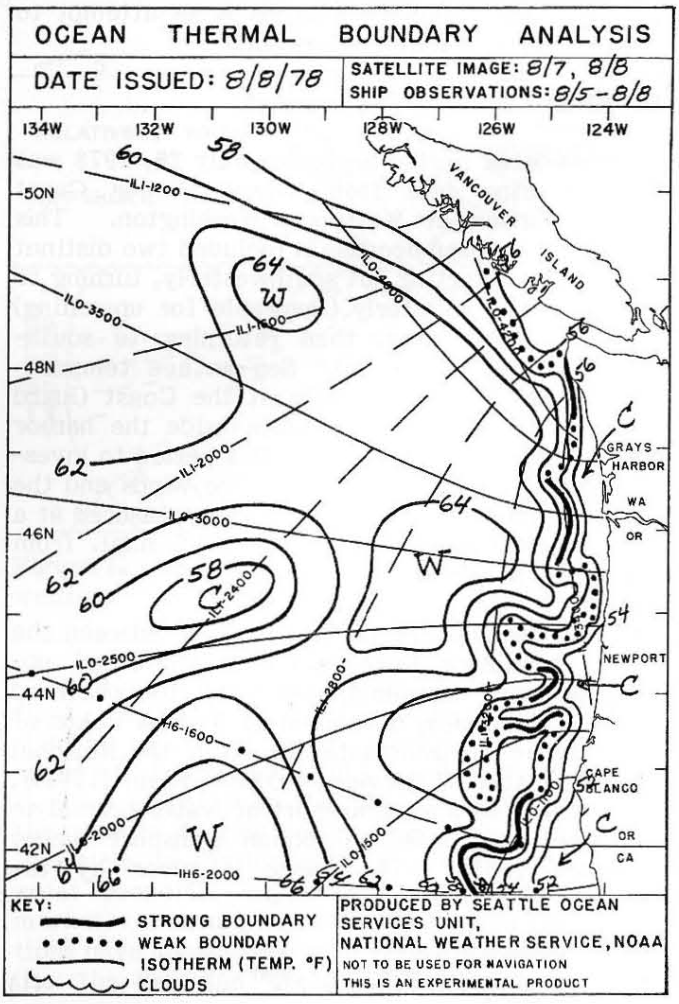

Figure 3. SOSU Ocean Thermal Boundary Analysis for 8 August.

and infrared satellite data also indicated that upwelling was well-established during this period. One of the enhanced IR VHRR images from NOAA-5 used in the analysis is also included (Figure 4). Notice the light grey shades (indicating cold water) along the coast all the way from Vancouver Island to northern California. The boundaries were highlighted in ink during the analysis.

It would have been desirable to examine some other parameters as well, such as nutrient and dissolved oxygen concentrations in the seawater (both indicators of upwelling) during this period, but such data are not routinely taken, and were unavailable.

III. CONCLUSIONS

The preceding analysis leads to the following conclusions:

(1) The wind direction and speed does appear to have an appreciable effect upon water temperatures along the Washington coast. This is presumably due to the coastal upwelling phenomenon.

(2) A lag exists between the wind forcing (as measured by the upwelling index) and the development of the observed response. For the case studied, this lage appears to be about 2.5 days; i.e. about 2-3 days after a north or northwest wind begins, a definite reduction of SST may be expected at Grays Harbor. Of course, this lag may vary, depending on such other factors as runoff and tidal current fluctuations.

(3) The cold water mass along the coast which results from the wind-induced upwelling is readily apparent on infrared satellite imagery and surface ship reports, which allows analyses to be drawn that can help fishermen locate productive areas more efficiently.

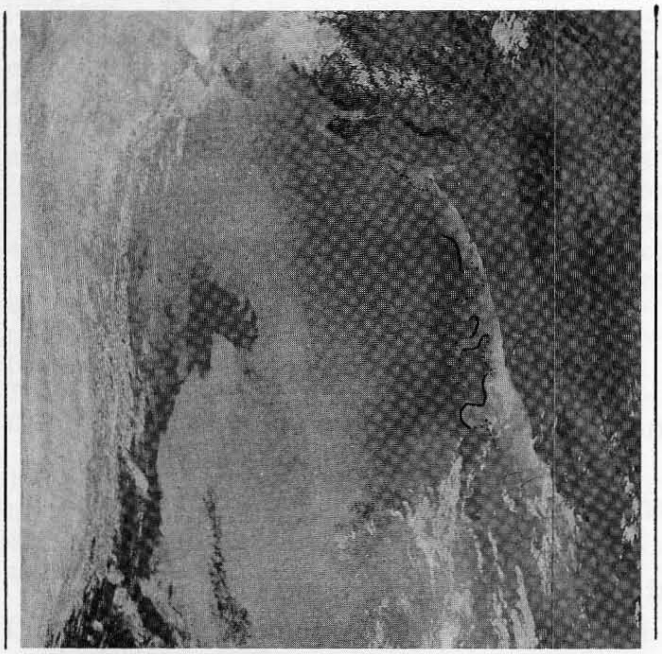

Figure 4. Enhanced infrared image from NOAA-5 for 7 August 1978, which was used in the analysis shown in Figure 3. Thermal boundaries were highlighted in ink during the analysis.

REFERENCES

Bakun, A. 1973. Costal upwelling indices, west coast of North America, 1946-1971. NOAA Tech. Rep. NMFS SSRF-671, 103 p.

Cannon, G. A. 1972. Wind effects on currents in Juan de Fuca Submarine Canyon. J. Phys. Oceanog. 2 (3): 281-285

Ekman, V. W. 1905. On the influence of the earth's rotation on ocean currents. Ark. f. Mat., Astron. och Fysik 2 (11): 1-53

Halpern, D. 1974. Summertime surface diurnal period winds measured over an upwelling region near the Oregon coast. Journ. Geophys. Res. 79 (15): 2223-2230.

Huyer, A.; R. D. Pillsbury; and R. L. Smith. 1974. Observations in a coastal upwelling region during a period of variable winds (Oregon coast, July, 1972). Tethys 6

Mommsen, D. B. 1978. The effect of surface wind on sea surface temperatures near Gibraltar. National Weather Digest 3 (4): 36-39.

Mooers, C. N. K.; C. A. Collins; and R. L. Smith. 1976. The dynamic structure of the frontal zone in the coastal upwelling region off Oregon. Journ. Phys. Oceanog. 6 (1): 3-21.

Smith, R. L. 1974. A description of current, wind and sea level variations during coastal upwelling off the Oregon coast, July-August 1972. Journ. Geophys. Res. 79 (3): 435-443

Stevenson, M. R.; R. W. Garvine; and B. Wyatt. 1974. Lagrangian measurements in a coastal upwelling zone off Oregon. Journ. Phys. Oceanog. 4 (3): 321-336

Thompson, J. D.; and J. J. O'Brien. 1973. Time-dependent coastal upwelling. Journ. Phys. Oceanog. 3 (1): 162-165

Quinn, W. H.; D. O. Zopf; K. S. Short; and R. T. W. Kuo Yang. 1978. Historical trends and statistics of the Southern Oscillation, El Nino, and Indonesian droughts. Fishery Bulletin 76 (3): 663-678.

APPENDIX A

Following is a brief and not fully rigorous outline of the theory from which the upwelling index is derived. See Ekman (1905) for complete details.

The simplified x and y momentum equations for ocean movement under wind forcing are:

$$fu = \frac{1}{\rho} \frac{\partial Ty}{\partial z} \quad (1)$$

$$fv = \frac{-1}{\rho} \frac{\partial Tx}{\partial z} \quad (2)$$

where

$f = 2\Omega \sin \phi$ (ϕ = latitude)

u, v = x, y velocity components of ocean movement

ρ = density

Tx, Ty - x and y frictional stress components

In order to simplify the problem, we rotate the x and y axes and define new axes x' and y' such that the y' axis is parallel to the local coastline. Then, we will only be interested in motion along the x' axis (offshore or onshore flow which causes upwelling or downwelling). Thus, only the x' momentum equation need be considered.

$$fu' = \frac{1}{\rho} \frac{\partial Ty'}{\partial z} \quad (3)$$

(u' = x' velocity component)

Since we are interested in a mass transport along the x' axis, equation (3) is rearranged so that a mass transport appears on the left-hand side:

$$\rho u' = \frac{1}{f} \frac{\partial Ty'}{\partial z} \quad (4)$$

In order to compute the integrated mass transport in the entire wind-driven layer, we next integrate equation (4) from Z = -D to Z = 0, where -D is defined as the depth at which the stress equals zero.

$$\int_{-D}^{0} \rho u' dz = \int_{-D}^{0} \frac{1}{f} \frac{\partial Ty'}{\partial z} dz \quad (5)$$

Defining M_x' as the vertically-integrated mass transport in the x' direction,

$$M_x' = \frac{1}{f} Ty' (z = 0) \quad (6)$$

However, Ty' (z = 0) is just the surface wind stress in the y' diretion. Therefore,

$$M_x' = \frac{1}{f} Ts \cos (D-C + 270^\circ) \quad (7)$$

where

Ts = surface wind stress in the direction the wind is blowing.

D = wind direction

C = coastline normal (directed offshore)

The cosine term in Equation (7) takes into account the rotation of the axes and the direction of the wind. The wind stress is given by:

$$Ts = \rho_a C_D V^2 \quad (8)$$

where

ρ_a = density of the air

C_D = drag coefficient

V = wind speed

ρ_a and C_D are taken to be constants for this computation. Making the assumption that the mass of water upwelled (or downwelled) is equal to the mass which moves offshore (or onshore), the upwelling index, U, is then:

$$U = M_x' = \frac{\rho_a C_D V^2}{2\Omega \sin \phi} \cos (D-C + 270^\circ) \quad (9)$$

or,

$$U = .288 \frac{V^2}{\sin \phi} \cos (D-C + 270^\circ) \quad (9)$$

The .288 factor incorporates all of the constants and conversion factors. The units of U are cubic meters per second per 100 meters of coastline. Equation (9) was used for the computations in this study.